

## Supporting Information

### Reactive Deposition of Nanofilms in Deep Polymeric Microcavities

Asif Riaz<sup>\*1,2,3</sup>, Ram P. Gandhiraman<sup>1</sup>, Ivan K. Dimov<sup>1,2</sup>, Lourdes Basabe-Desmonts<sup>1</sup>, Jens Ducreé<sup>1</sup>,  
Stephen Daniels<sup>1</sup>, Antonio J. Ricco<sup>1</sup>, and Luke P. Lee<sup>\*1,2</sup>

<sup>1</sup>*Biomedical Diagnostics Institute, National Centre for Sensor Research,  
Dublin City University, Glasnevin, Dublin, IRELAND*

<sup>2</sup>*Biomolecular Nanotechnology Center, Berkeley Sensor and Actuator Center, Department of  
Bioengineering, University of California, Berkeley, CA, USA*

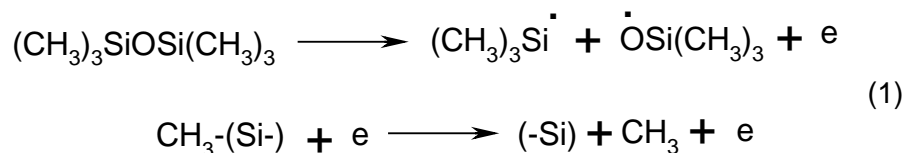
<sup>3</sup>*Nano Bio-Solution Inc., 168, Street 54, I-8/3, Islamabad, Pakistan*

## Contents

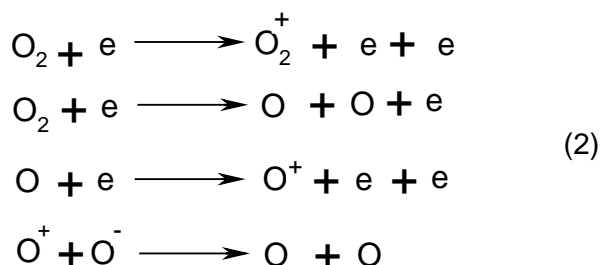
SI-1 Reaction mechanisms.....	2
SI-2 Plasma chamber and reaction setup.....	2
SI-3 Optical emission spectroscopic diagnostics of the plasma.....	4
SI-4 Concentration profiles of gas in the microcavities. ....	4
SI-5 Cross sectional view of a micro cavity filled with RhB solution .....	6
SI-6 Effect of HMDSO on barrier film formation .....	6
SI-7 Atomic force microscopy images of bare and SiO <sub>x</sub> barrier film on PDMS.....	6
SI-8 Long Term stability of SiO <sub>x</sub> coating against toluene exposure .....	7
SV-1 Effect of cross sectional area on barrier film efficiency.....	7
SV-2 Resistance to toluene .....	7
References.....	7

## SI-1 Reaction mechanisms

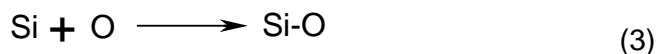
Hexamethyldisiloxane (HMDSO) and oxygen were introduced into plasma chamber using a controlled flow rate, usually at 16 sccm and 500 sccm, respectively. According to the widely accepted mechanism<sup>[1]</sup>, in high power plasma (300 W) the dissociation of HMDSO into its fragments is expected as given below:



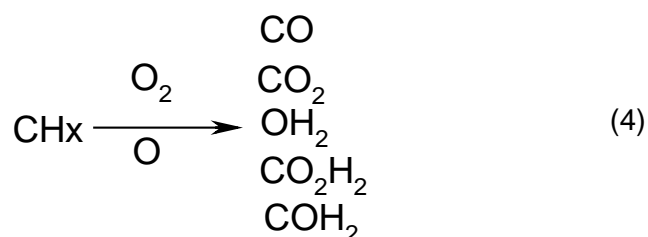
The impact of electrons on the precursor molecules results in the formation of highly reactive ions, radicals and metastable species. The molecular oxygen introduced into the plasma-environment fragments into molecular and elemental ions as well as elemental oxygen as proposed<sup>[2]</sup> in the following equations:



The reaction of oxygen with the fragments of HMDSO leads to formation of Si and O radicals. Since the charged species oscillate with the RF power in the plasma, we propose that neutral radicals of Si and O are more likely to migrate into the microcavities by diffusion. The following reaction of Si and O radicals is suggested in the microcavities resulting into glass like thin film of SiO<sub>x</sub>.



In plasma environment, the presence of highly reactive species like hydrogen and oxygen could be established using optical emission spectroscopy as shown in Fig. SI-3. The hydrocarbon containing fragments of HMDSO produced in the plasma react with the fragments of O<sub>2</sub> resulting into the formation of formaldehyde, formic acid, carbon oxide, carbon dioxide and water<sup>[3]</sup>. The presence of higher amount of oxygen content in the plasma will lead to reduced carbon content in the barrier.



## SI-2 Plasma chamber and reaction setup

SiO<sub>x</sub> barrier formation reaction was performed in a computer controlled plasma reactor from Europlasma Inc., model CD300 (Oudenaarde, Ghent, Belgium). A schematic diagram of the system is shown in Fig. SI-2. The aluminium chamber of the system was connected to a Dressler's CESAR 136 RF power source at 13.56 MHz (Munsterau, Stolberg, Germany) supplied with an automated impedance

match-box for effective RF energy input to the plasma. Pressure in the chamber was measured using an MKS Baratron type absolute pressure transducers Granville-Phillips gauge (Andover, MA, USA). BOC Edwards EH mechanical booster pump (Crawley, West Sussex, UK) backed by an Edwards High Vacuum International E1M40 rotary pump (Crawley, West Sussex, UK), was used to pump down the chamber, which was connected through a duct at the bottom of the chamber. The powered electrode (PE), a conducting plate (24 cm x 21 cm with a 6 cm diameter hole in the middle) was placed slightly below ceiling piece of the chamber. An electrically isolated hollow metallic setup (24 cm x 21 cm x 1.2 cm) was used as the sample stage, which was placed 10 cm beneath PE. Our PDMS samples bearing microcavities were placed on the sample stage for the SiO<sub>x</sub> barrier film formation. The mass flow controllers (MFCs) were used to control the flow of gases, which were equipped with shut off valves to avoid leakage of any gas being not in use during the process. Plasma environment was generated by turning on the input RF current/voltage to PE while the chamber walls were kept in grounded state. In the plasma, free electrons and ions are accelerated by the electric field, and collide with the molecules of the source gases exciting them to higher energy states. The collisions of the energetic electrons are primarily inelastic in nature, which dissociate the molecules into a variety of radicals, ions, atoms and more electrons.

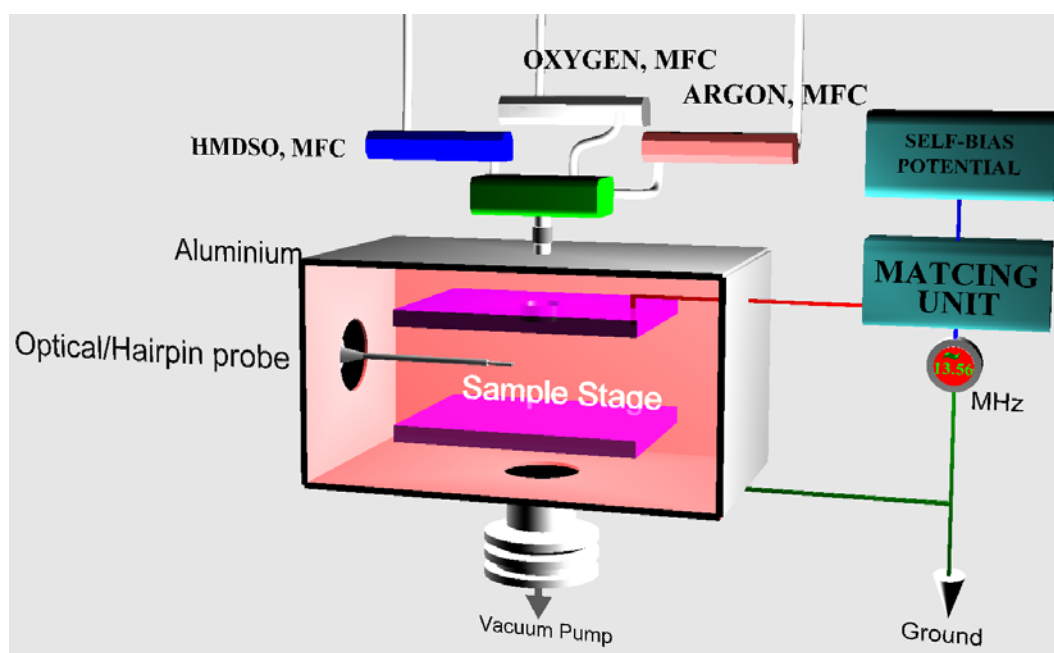


Figure SI-2. Schematic diagram of RF plasma chamber used for the SiO<sub>x</sub> barrier film formation in the microcavities.

The dissociation of precursor HMDSO molecule takes place by electron impact followed by oxidation of the fragments by atomic oxygen<sup>[1]</sup>. The reactive species generated in the plasma travel to the growing film surface through a gas phase diffusion process, and adsorbed onto the surface to form chemical bonds at favourable sites to raise an amorphous network. Creatore et al., observed that at oxygen to HMDSO ratios greater than 10, more homogeneous SiO<sub>x</sub> radicals are produced and the film property approaches to that of silica-like<sup>[4]</sup>. Magni et al., reported that at oxygen to HMDSO ratios > 30, oxygen chemistry is dominant in the plasma<sup>[3]</sup>. The plasma electron density measured using a floating microwave hairpin resonance probe was found to be  $0.154 \times 10^{10} \text{ cm}^{-3}$  during our SiO<sub>x</sub> barrier film formation (in conditions as described in Fig. 2, main text).

### SI-3 Optical emission spectroscopic diagnostics of the plasma

The plasma diagnostics were carried out by means of optical emission spectroscopy as shown in Fig. SI-3. A UV transparent window was fixed at the side port of the chamber and the light emitted by the plasma was collected by an optical fibre and directed towards the Ocean Optics HR4000 (Dunedin, FL, USA) high resolution spectrometer. The HR4000 has a 3648-element CCD-array detector from Toshiba® that enables optical resolution as precise as 0.02 nm (FWHM). The HR4000 is responsive from 200-1100 nm. The optical emission spectroscopy (OES) reveals the presence of hydroxyl groups, elemental oxygen (O), hydrogen (H), silicon radical (Si), carbon monoxide (CO) and hydrocarbon species. The emissions of SiO radical occurring at 241.3 nm could not be measured.

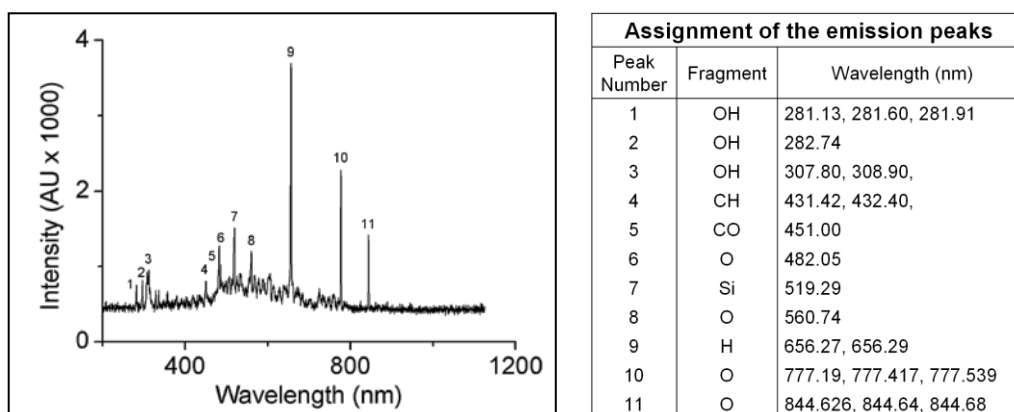


Figure SI-3. Optical emission spectroscopy of plasma fed with O<sub>2</sub> and HMDSO. Spectrum of the plasma (left) and assignment of the peaks (right). Plasma conditions: 300 W, O<sub>2</sub> 500 sccm, HMDSO 16 sccm, and pressure 300 mTorr.

The atomic species like hydrogen, carbon and oxygen produce bigger organic molecules like formaldehyde or carbon dioxide etc were also present. The breakdown of the monomers is evident from this OES study. The highly reactive radicals and atomic species could result in oxidation of the hydrocarbons in the precursor resulting in formation of H<sub>2</sub>O, formic acid, formaldehyde and CO<sub>2</sub>, which were sucked out of the system by the vacuum pump.

### SI-4 Concentration profiles of gas in the microcavities.

Concentration profiles of an arbitrary reaction were generated by 2-dimensional computer simulation, where gaseous atoms adsorb on the surface in a microcavity. Figure SI-4 shows surface concentration of the adsorbed species from  $t = 0.5$  s to  $t = 6$  s. It shows that as the adsorption time increases so does the amount of the adsorbed species. As the gaseous molecules enter the microcavity a clear exponential decay is seen in the surface concentration from the inlet towards the inside of the microcavity. The inset shows bulk concentration of species in the microcavity from  $t = 0$  s to  $t = 6$  s. Steady state is reached at approx. 2 s. This dynamics is very similar to the one measured experimentally (see Fig. 2c–d, main text) for thickness of the barrier film along the microcavity length with respect to reaction time and chamber pressure, suggesting that SiO<sub>x</sub> barrier film formation process follows dynamics based on reactant particles migrating into the microcavities by diffusion and then reacting on the surfaces inside the microcavities. The microcavity in this study is 100 μm wide and 1 mm long.

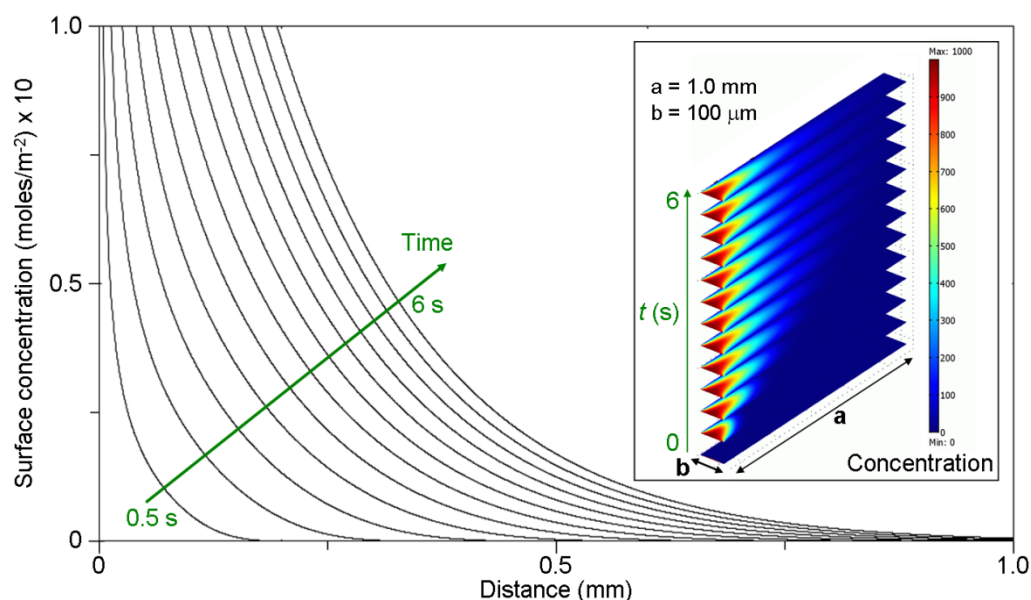


Figure SI-4. Diffusion based surface concentration profiles along the length of the microcavities at various times. Gas concentration profiles with distance in a microcavity (Inset) of 100 μm width and 1 mm. Qualitative two dimensional simulations were performed using COMSOL v3.3 software.

### Simulation parameters

All simulations were done on COMSOL Multiphysics v3.3 (COMSOL Ltd., Hertfordshire, UK). The simulation models are based on the material balance for the surface, including surface diffusion and the reaction rate expression for the formation of the adsorbed species,  $c_s$ . This results in the following expression:

$$\frac{\partial c_s}{\partial t} + \nabla \cdot (-D_s \nabla c_s) = k_{ads} c (\theta_0 - c_s) - k_{des} c_s$$

Where,  $D_s$  represents the surface diffusivity,  $k_{des}$  the rate constant for the backward reaction,  $k_{ads}$  the rate constant for the forward reaction,  $c_s$  the surface concentration of adsorbed species,  $\theta$  the surface concentration of active sites, and  $c$  the bulk concentration.

The concentration of the bulk species,  $c$  is solved in combination with the mass balance in the bulk given by:

$$\frac{\partial c}{\partial t} + \nabla \cdot (-D \nabla c + c \mathbf{u}) = 0$$

Where,  $D$  denotes the diffusivity of the reacting species,  $c$  the bulk concentration, and  $\mathbf{u}$  the velocity vector.

The coupling between the mass balance in the bulk and the surface is done as a boundary condition in the bulk's mass balance by setting the flux of  $c$  at the boundary equal to the rate of the surface reaction.

### Initial and Boundary Conditions

At  $t = 0$ ,  $c_s = 0$ ,

Inlet:  $c = c_0$

Outlet:

$$\mathbf{n} \cdot (-D \nabla c + c \mathbf{u}) = \mathbf{n} \cdot c \mathbf{u}$$

Active surface:

$$\mathbf{n} \cdot (-D \nabla c + c \mathbf{u}) = k_{ads} c (\theta_0 - c_s) - k_{des} c_s$$

### Estimated constants

$$c_0 = 1000 \text{ moles} / \text{m}^3, k_{ads} = 1 \times 10^{-6}, k_{des} = 1 \times 10^{-9},$$

$$\theta_0 = 1000, D_s = 1 \times 10^{-11}, D = 1 \times 10^{-9}$$

The simulation was done until the bulk concentration reached a steady state (in approx. 6 s). The surface concentration of the adsorbed species decays exponentially from the inlet into the cavity and increases proportionally with the adsorbing time.

### SI-5 Cross sectional view of a micro cavity filled with RhB solution

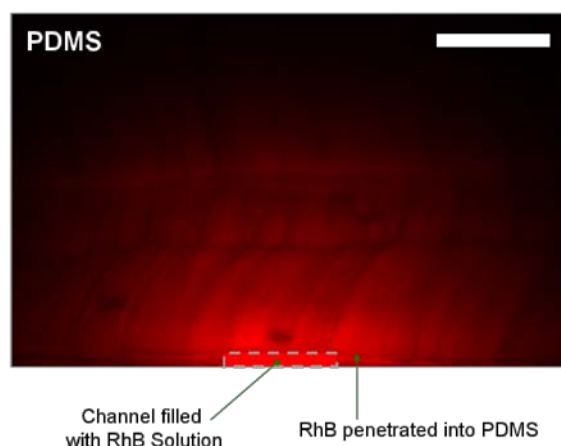


Figure SI-5. Cross sectional view of RhB-fluorescence in bare PDMS. A sliced section of PDMS where RhB solution ( $10\ \mu\text{M}$ ) was stored for 3 hrs. The red fluorescence outside the dotted line in the image is due to RhB molecules penetrated into PDMS through the walls. The dotted line shows the microchannel cross sectional boundary and the red colour inside the dotted line depicts the RhB solution confinement area. ( $30\ \mu\text{m} \times 300\ \mu\text{m} \times 10\ \text{mm}$ ). Scale bar  $300\ \mu\text{m}$ .

### SI-6 Effect of HMDSO on barrier film formation

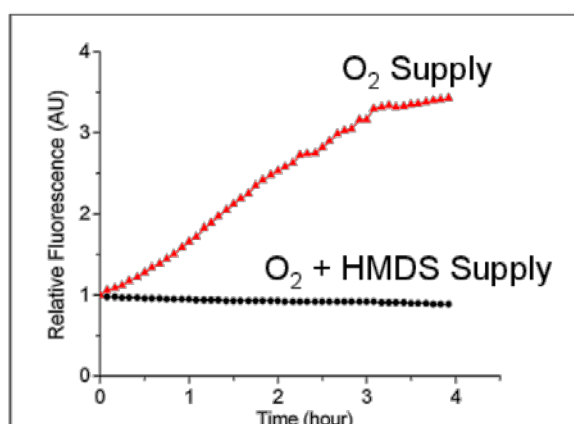


Figure SI-6. Effect of HMDSO on barrier film formation.  $\text{SiO}_x$  barrier film formation in PDMS microcavities was tested in the absence of HMDSO where Si radicals were not available from the external source except O. The experiments reveal that HMDSO is a necessary precursor for the barrier film, O radicals could not form a permanent  $\text{SiO}_x$  barrier by the oxidation of the PDMS surface. RhB-fluorescence with time along the microcavities treated in the absence of HMDSO (red triangles) and in the presence of HMDSO (black circles). The barrier formation conditions: RF power 300 W, time of reaction 40 min, and operating pressure 300 mTorr. Dimensions:  $50\ \mu\text{m}$  wide,  $100\ \mu\text{m}$  high and 2 cm long.

### SI-7 Atomic force microscopy images of bare and $\text{SiO}_x$ barrier film on PDMS

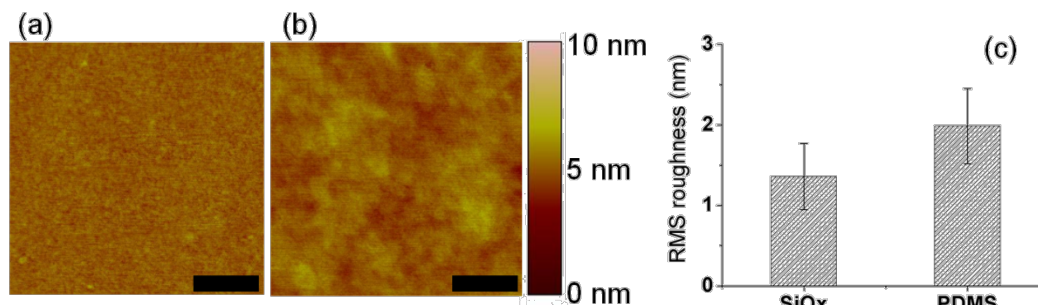


Figure SI-7. AFM images of Bare and  $\text{SiO}_x$  barrier film on PDMS. Atomic force microscopy (AFM) examinations were performed with a Dimension 3100 AFM (Swavesey, Cambridge, UK) using a Nanoscope IIIa controller equipped with a phase imaging extender (Digital Instruments, Bala, Gwynedd, UK) operating in tapping-mode (TM-AFM). Standard silicon tips (Tap300Al, BudgetSensors, Phoenix, AZ, USA) were used with 42 N/m nominal spring constant and 300 kHz nominal resonance frequency. All images were recorded in air at room temperature, at a scan speed of 1 Hz. The images were flattened using second-order flattening routines to remove any sample tilt and/or curvature before obtaining root-mean-square (rms) roughness values. No further filtering was performed. Roughness values presented are averaged values



obtained from three different measurements on 20  $\mu\text{m}$  x 20  $\mu\text{m}$  images. Tapping Mode™ AFM images of (a) untreated PDMS, and (b)  $\text{SiO}_x$  barrier film on PDMS, showing the surface topography before and after the film formation. Scale bar 50 nm. (c) RMS roughness values of the untreated and  $\text{SiO}_x$  barrier film on PDMS samples (area 2  $\mu\text{m}$  x 2  $\mu\text{m}$ ).

### SI-8 Long Term stability of $\text{SiO}_x$ coating against toluene exposure

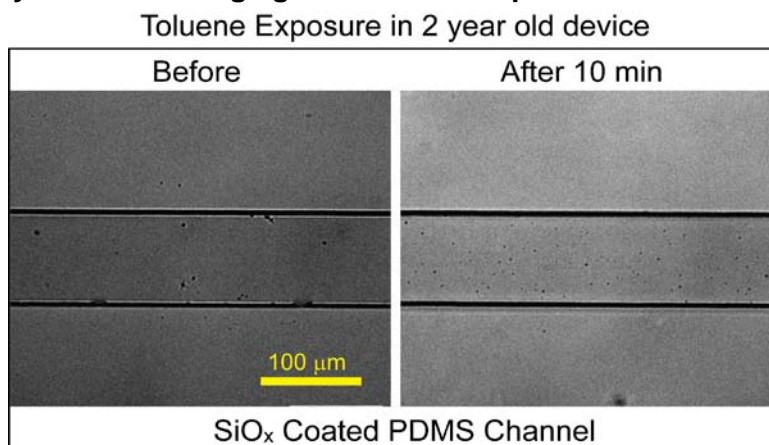


Figure SI-8. Toluene was filled in a device bearing about 2 year old  $\text{SiO}_x$  coating. The barrier formation conditions: RF power 300 W, time of reaction 40 min, and operating pressure 300 mTorr. Dimensions: 50  $\mu\text{m}$  wide, 100  $\mu\text{m}$  high and 2 cm long.

### SV-1 Effect of cross sectional area on barrier film efficiency

**Video clip 1:** Cross section 250  $\mu\text{m}^2$  (10 x 25); format: avi

**Video clip 2:** Cross section 750  $\mu\text{m}^2$  (10 x 75); format: avi

**Video clip 3:** Cross section 1,500  $\mu\text{m}^2$  (30 x 50); format: avi

**Video clip 4:** Cross section 9,000  $\mu\text{m}^2$  (90 x 100); format: avi

### SV-2 Resistance to toluene

**Video clip 4:** Toluene in bare PDMS channel; format: avi

**Video clip 5:** Toluene in  $\text{SiO}_x$  barrier film PDMS channel; format: avi

### References

- [1] M. Goujon, I. Belmonte, G. Henrion, *Surf. Coat. Technol.* **2004**, 188, 756-761.
- [2] A. Yanguas-Gil, J. Cotrino, A. R. Gonzalez-Elipse, *J. Phys. D-Appl. Phys.* **2007**, 40, 3411-3422.
- [3] D. Magni, C. Deschenaux, C. Hollenstein, A. Creatore, P. Fayet, *J. Phys. D-Appl. Phys.* **2001**, 34, 87-94.
- [4] M. Creatore, F. Palumbo, R. d'Agostino, *Plasmas Polym.* **2002**, 7, 291-310.